1 Introduction

Plasma is an ionized state of matter whose main constituents are electrons and ions. It is the most predominant state of visible matter in the universe. There are various parameters that define the characteristics of a plasma such as characteristic frequency and Debye length. A characteristic frequency of plasma oscillations is the electron plasma frequency $\omega_p = (ne^2/m\varepsilon_0)^{1/2}$, where n, $-e$, and m are the electron number density, charge, and mass, respectively and ε_0 is the vacuum electric permitivity. According to linear theory, an electromagnetic wave of frequency ω normally incident on a plasma slab is reflected at the critical layer where $\omega = \omega_p$. For waves of higher frequency, $\omega > \omega_p$, the plasma behaves as an optically transparent medium with the refractive index $\eta = \left(1 - \omega_p^2 / \omega^2\right)^{1/2}$. Electron and ion collisions cause the wave to be damped.

There also exists a characteristic length in a plasma, the electron Debye length $\lambda_D = v_{\text{th}}/\omega_p$, where $v_{\text{th}} = \sqrt{T_e / m}$ is the electron thermal speed, and T_e is the electron temperature in energy units. The electron Debye length characterizes the length over which the electric potential of a charged particle is screened by the electrons and ions of the plasma. An ionized gas of size much greater than λ_D can be called a plasma. The screening of the potential is crucial for the description of the dynamics of charged particles, otherwise the electric and magnetic fields produced by each charged particle would influence the motion of all the other particles (billions and billions in number) and each one would move in the fields of all others. The Debye screening localizes the micro-fields of the individual particles to within a Debye sphere, containing a large number of particles $N \approx n\lambda_D^3 >> 1$, where N is called the plasma parameter.

At a distance of a Debye length, the potential energy of a particle equals its kinetic energy, and beyond that the latter prevails. The quantity $1/N$, provides us an expansion parameter, valid to the zeroth order, in which one can neglect the correlations and collisions of charged particles. This is called the Vlasov approximation. Binary collisions are an effect to the next order.

https://doi.org/10.1017/9781108635844.002 Published online by Cambridge University Press

1.1 Laser Produced Plasma

A high power laser is an effective means of producing high density plasma on a nanosecond, pico-second, or even femto-second time scale with a temperature greater than 100 electronvolts (eV). Most laser–plasma experiments employ Nd:glass lasers (1.06 μm) or Ti:Sapphire lasers (0.8 μm) on targets that include gas jets or thin foils or spherical pellets. Experiments with CO_2 lasers (10.6 μm) have also been conducted.

1.1.1 Tunnel ionization

A striking feature in using lasers at high intensities (> 10^{14} W/cm^2) is the process of tunnel ionization that produces plasma on sub pico- second time scales. As Keldysh[1] showed, the rate of tunnel ionization of atoms caused by the electric field E of a laser with frequency ω is

$$\gamma = (\pi/2)^{1/2}(I_0/\hbar)(|E|/E_A)^{1/2}\exp(-E_A/|E|), \tag{1.1}$$

where $E_A = (4/3)(2m)^{1/2} I_0^{3/2}/e\hbar$ is the characteristic atomic field, I_0 is the ionization energy, and $\hbar$ is the reduced Planck's constant. This expression is written in the limit when the electron quiver energy $mv_0^2/2 > I_0$. Here $v_0 = e|E|/m\omega$ is the amplitude of the electron quiver velocity due to the laser. One may write $mv_0^2/2 = 1500 P_{16}\lambda_\mu^2$ in eV where P_{16} is the laser intensity in units of 10^{16} W/cm^2 and λ_μ is the laser wavelength in microns. At a lower laser intensity, plasma is produced via impact ionization. Plasma produced locally, with size r_0, undergoes ambipolar diffusion on the time scale of $\tau_d = r_0/c_s$, where $c_s = \sqrt{T_e/m_i}$ is the ion sound speed and m_i is the ion mass.

1.1.2 Impact ionization

Impact ionization is a process in which a laser, shining on a target, heats the seed electrons (produced via tunneling or some other process). Heating involves collisions between the electrons and atoms or ions, without which the electron current density is $\pi/2$ out of phase with the laser field and there is no time average heating. In a collision, the momentum of an electron is randomized but only a small fraction of the energy (of the order of twice the electron to atom mass ratio) is exchanged. A collision does two things – it provides an in-phase component to the current density with the electric field and raises the thermal energy of electrons. As the kinetic energy of the electrons exceeds the ionization energy of the atoms, the electrons ionize the atoms on colliding with them, at the rate

$$\partial n_e/\partial t = \alpha n_a n_e, \tag{1.2}$$

where n_a is the number density of neutral atoms, n_e is the number density of electrons, and α is the coefficient characterizing the ionizing collisions. The process grows exponentially in time.

https://doi.org/10.1017/9781108635844.002 Published online by Cambridge University Press

The collision cross-section for impact ionization rises with the temperature T_e (in energy units) as $\exp(-I_0/T_e)$, hence, higher the intensity of the laser, higher the heating rate and higher the rate of ionization. In atoms with many electrons, the ionization energy to reach a singly ionized state is the lowest and it increases with the state of ionization.

Not all collisions are ionizing – some are elastic collisions, and some raise the atoms to excited states (called Rydberg states whose orbital radii are proportional to the square of the number of the state). The atoms in excited states stay there for a significant time and have a much higher collision cross-section for ionizing collisions, They play an intermediary role in ionization when the electron energy is less than the ionization energy. In one collision, the atom goes to a Rydberg state and in the next collision it becomes ionized. Sharma et al.[2] have observed up to seven states of ionization of Xe using nano-second pulses of moderate energy, ~10^9 W/cm^2. Rajeev et al.[3] have employed high cross-section of Rydberg states to induce charge exchange collisions of ions with atoms for the production of high energy atoms.

1.2 Electromagnetic and Electrostatic Waves

An unmagnetized plasma supports three principal kinds of waves: electromagnetic wave with the dispersion relation $\omega = \left(\omega_p^2 + k^2c^2\right)^{1/2}$, a low-frequency ion-acoustic wave with $\omega = kc_s/\left(1 + k^2v_{\text{th}}^2/\omega_p^2\right)^{1/2}$, and a high frequency Langmuir wave with $\omega = \left(\omega_p^2 + 3k^2v_{\text{th}}^2/2\right)^{1/2}$, where ω is the angular wave frequency and k is the wave number. The ion-acoustic and Langmuir waves are Landau damped when their phase speed ω/k is low enough to interact resonantly with the ions and electrons, respectively. The ion-acoustic wave is strongly Landau damped on ions unless the electron temperature is much higher than the ion temperature; the Langmuir wave becomes strongly Landau damped at short wavelengths due to the resonant interaction with electrons.

The presence of density gradient in the plasma brings about the novel phenomenon of mode conversion. It is especially important for an electromagnetic wave that is obliquely incident onto an inhomogeneous plasma with the electric field component along the density gradient. The wave then drives a density oscillation. At the critical density $n = n_c = m\varepsilon_0\omega^2/e^2$, the driven density oscillation is an electron plasma (Langmuir) wave. Thus, an electromagnetic wave energy can be directly converted to the Langmuir wave through "resonance absorption", and is eventually absorbed by the plasma. This is an example of how modes and resonant mode coupling are important for the absorption of electromagnetic waves in plasma.

1.3 Parametric Instabilities

For a large-amplitude electromagnetic wave, the nonlinear coupling with the electrostatic modes, caused by parametric instabilities becomes dominant.[2–12] These couplings can occur in the underdense region as well as near the critical layer. In an underdense plasma,

https://doi.org/10.1017/9781108635844.002 Published online by Cambridge University Press

an electromagnetic wave can decay into another electromagnetic wave and an electrostatic wave, that is, a Langmuir wave or the ion-acoustic wave, resulting in stimulated Raman and Brillouin scattering, respectively. Near the critical density the electromagnetic wave can decay into a Langmuir wave and an ion-acoustic wave. The energy of the electromagnetic wave is then diverted to the electrostatic modes, which in turn can heat the particles through Landau damping and collisions. The nonlinear interaction of electromagnetic waves with collective modes in the plasma, therefore, qualitatively changes the nature of its propagation, absorption, and scattering. Plasma inhomogeneity plays an important role in these parametric wave–wave interactions. It limits the region of resonant wave–wave coupling, and enhances the threshold for parametric instabilities.

There exist comprehensive texts treating many aspects of electromagnetic waves in plasmas.[6–8] This monograph aims at reviewing the physical processes of the linear and nonlinear collective interactions of electromagnetic waves with unmagnetized plasmas. We have several specific applications in mind, including laser-driven-fusion and advanced electron and proton accelerators.

1.4 Laser Driven Fusion

Laser-driven inertial confinement fusion (ICF) is a major scientific challenge. It aims at heating and compressing a deuterium–tritium (D–T) target using an intense laser light at temperatures above 10 keV and superhigh density. The D–T nuclei undergo an exothermic fusion reaction producing energy. The basic fusion reaction is as follows.

$$ {}_1\mathrm{D}^2 + {}_1\mathrm{T}^3 \rightarrow {}_2\mathrm{He}^4 + {}_0 n^1 + 17.6\ \mathrm{MeV}. \tag{1.3} $$

Deuterium is available in abundance in sea water, in the form of D_2O, and can be extracted at reasonable cost. Tritium can be obtained from lithium, available widely in the soil through neutron bombardment.

$$ {}_3\mathrm{Li}^6 + {}_0 n^1 \rightarrow {}_2\mathrm{He}^4 + {}_1 \mathrm{T}^3. \tag{1.4} $$

The Lawson criterion for energy breakeven, that is, when the energy produced via thermonuclear fusion equals the energy employed in plasma production and heating, requires at 10 keV plasma temperature the product of density and plasma confinement time $n\tau > 10^{14}$ cm^{-3} sec. For inertial confinement, τ is the ambipolar diffusion time $\tau_d = r_0/c_s$, required for the sound wave to traverse a microsphere of radius r_0 of a few hundred microns; thus, the densities required are about thousand times higher than a normal solid density. This is achieved by shock compression of spherical D–T targets using the laser itself or by laser induced X-rays. There are two approaches to ICF: direct-drive and indirect-drive.

https://doi.org/10.1017/9781108635844.002 Published online by Cambridge University Press

1.4.1 Direct-drive ICF

In direct-drive ICF, the laser deposits its energy in the corona, that is, the underdense region and the critical layer via collisional and resonance absorption. The heat is transported to the ablation layer by thermal conduction where a shock wave is generated. This shock wave compresses the core. The target capsule (3–5 mm in radius) comprises D–T gas at the core, surrounded by cryogenic D–T ice (thickness 160–600 μm) inside a CH shell. Multi-beam laser (e.g., 192 beams in the National Ignition Facility (NIF) at Lawrence Livermore Laboratory) of 0.351 μm wavelength and nanosecond pulse length symmetrically irradiates the spherical capsule. Craxton et al.[13] have in an extensive review article divided the implosion into four phases (cf. Fig. 1.1). At first, the laser is absorbed by the target, leading to the formation of a hot plasma corona and the ablation of the target (at the ablation surface). Suitably tailored laser pulses produce a sequence of shock waves that propagate into the target. After the shock has reached the inner surface, a rarefaction wave moves outward toward the ablation surface, and the shell begins to accelerate inwards towards the target center. The laser intensity increases during the accelerating phase up to ~10^{15} W/cm^2. After the main shock wave reflects from the target center and reaches the shell/D–T layer, a deceleration phase begins and the kinetic energy of the shell is converted into thermal energy, leading to that the D–T fuel is compressed and heated.

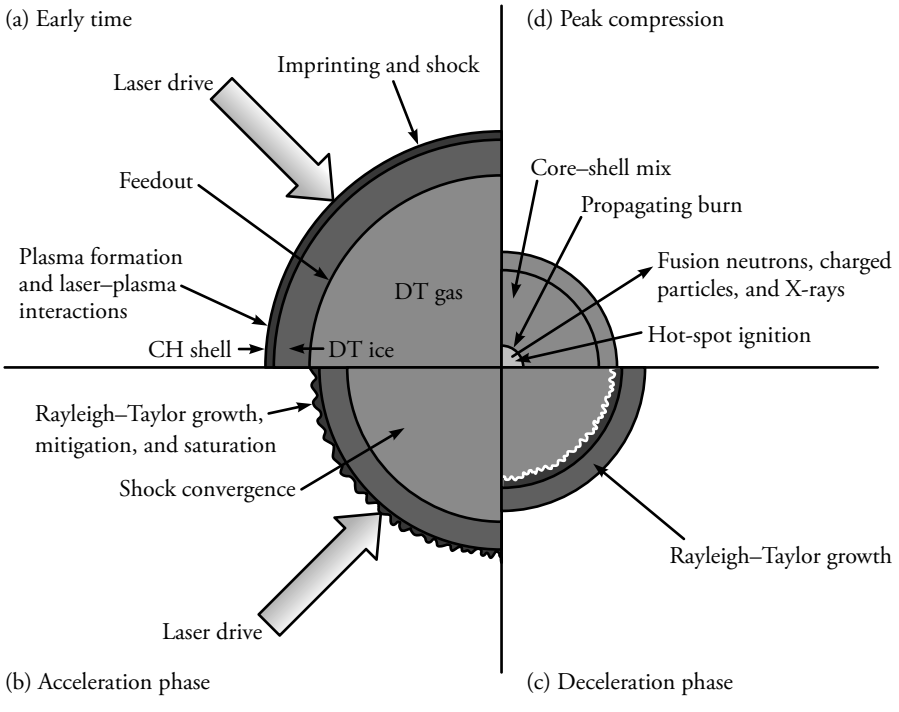

Fig. 1.1 Different stages of implosion in direct-drive fusion as shown by Craxtom et al.[13]

https://doi.org/10.1017/9781108635844.002 Published online by Cambridge University Press

During the deceleration phase, the Rayleigh–Taylor instability is a serious concern as it may destroy the symmetry and inhibit compression. Peak compression occurs in the final phase when fusion neutrons and X-rays are produced along with α particles. These particles deposit energy in the D–T fuel bringing more compressed fuel to the fusion temperature and leading to a propagating burn (ignition). A 10 keV temperature and a compressed mass density to the radius product of ρR = 300 mg/cm^2 are required for ignition.

1.4.2 Indirect-drive ICF

In indirect drive ICF, the D–T filled capsule is placed at the center of a cylindrical enclosure (a hohlraum) coated on the interior with a high-Z material , for example, gold (see Fig. 1.2). The inside wall of the hohlraum is irradiated using multi-beam lasers. This produces X-rays which ablate the fuel filled capsule. The lasers are launched into outer cones and inner cones, through the entrances at the ends to maintain an X-ray flux symmetry at the poles and equator of the capsule.[14,15] Typical experiments at NIF utilize hohlraums filled with helium at densities in the range 0.96–1.6 mg/cm^3 to minimize the expansion of the interior high–Z gold wall, and help the laser reach the wall for the full pulse duration. The laser turns the gas inside the hohlraum to a low density plasma ($n/n_{cr} \leq 0.1$) with the electron temperature $T_e \sim 3$ keV.

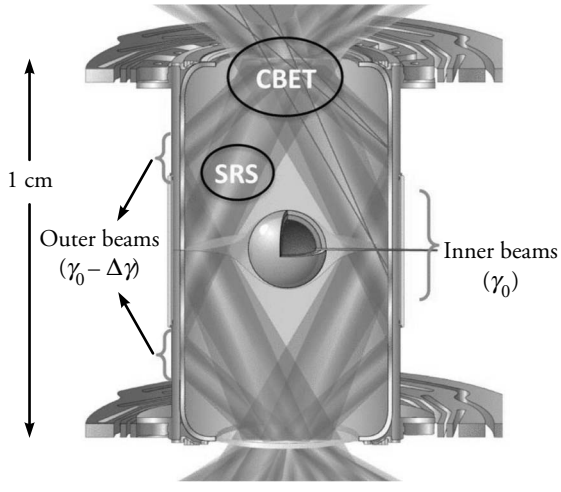

Fig. 1.2 Indirect-drive fusion: Hohlraum carrying a spherical D–T capsule in the center. Multi-laser beams enter through the end entrances, irradiate the gold-coated hohlraum wall as inner and outer beams and produce X-rays that cause implosion of the capsule. Cross-beam energy transfer (CBET) may take place at the entrance. (cf. Montgomery.[14])

The nonlinear interaction of intense laser light with the corona plasma is primarily due to parametric instabilities. Below the critical density, the laser excites large amplitude Langmuir and ion-acoustic waves, through the parametric Raman and Brillouin scattering instabilities.

https://doi.org/10.1017/9781108635844.002 Published online by Cambridge University Press

These waves can produce high-energy electrons and ions, respectively, that can preheat the core and diminish the efficiency of shock compression.

1.5 Charged Particle Acceleration

The early work of Rosenbluth and Liu[16] on the beat wave excitation of high amplitude high phase velocity Langmuir waves by two collinear lasers in a plasma and that of Tajima and Dawson[17] on wake-field excitation by a short pulse laser (of pulse duration ω_p^{-1}) initiated extensive studies on electron acceleration by large amplitude plasma waves. In these experiments, a gas jet target is impinged by a short pulse laser. The front of the pulse creates a plasma and the remainder of the pulse drives a wake-field plasma wave. The phase velocity of the plasma wave equals the group velocity of the laser. The plasma wave traps energetic electrons and accelerates them to GeV energy. At higher laser intensity, one obtains an electron evacuated ion bubble in the wake of the laser. In the moving frame of the bubble, electrons travel backward on the periphery of the bubble and surge to the stagnation point. The ion space charge field pulls these electrons into the bubble, accelerating them to GeV energies.

High power laser interaction with thin foil targets has opened up the possibility of proton acceleration via radiation pressure acceleration (RPA). A laser of intensity I_L carries I_L/c momentum per unit area per second. After being reflected from an overdense plasma foil, the laser exerts $2I_L/c$ radiation pressure or ponderomotive force on the plasma electrons. As the electrons move, the ion space charge left behind pulls them back, creating a double layer. The latter is accelerated by the radiation pressure as a whole, only limited by the Rayleigh–Taylor (RT) instability. Particle-in-cell (PIC) simulations with foils of two ion species,[18] reveal that a proton layer can detach from the heavier ions and the RT instability is mainly localized to the heavier ions. Experiments with diamond-like carbon (DLC) foils of 2–5 nm thickness, with adsorbed hydrogen on the rear, have resulted in proton energies of the order of 60 MeV. One considers the possibility of achieving quasi-mono-energy ion beams of 200 MeV energy in the near future. It would be a major breakthrough for cancer therapy.

If thicker foils are used, the electrons in the skin layer are pushed by the ponderomotive force to the rear where they create a high field sheath. The sheath accelerates adsorbed protons via the target normal sheath acceleration (TNSA) process.

1.6 Coherent X-rays

Laser produced plasmas are also useful sources of coherent radiation, for example, terahertz generation, harmonic generation, X-ray laser, and gamma ray generation. The mechanisms of X-ray laser and gamma ray generation are based on the same principles as a free electron laser (FEL). In an FEL,[18–23] a relativistic electron beam propagates through a periodic transverse magnetic field called a wiggler. The wiggler appears to the beam as an incoming electromagnetic wave whose stimulated Compton backscattering produces double Doppler-shifted coherent

https://doi.org/10.1017/9781108635844.002 Published online by Cambridge University Press

radiation. In this process, the wiggler and the radiation seed signal exert a ponderomotive force on the electrons causing space charge bunching and emission of coherent radiation. The wavelength of the radiation is proportional to the wiggler period and inversely proportional to the square of the energy of the beam. Currently, there is a growing need for employing lasers as wigglers and laser accelerated electrons as the beam that upconverts the laser to hard X-rays and gamma rays. The electrostatic field of the laser produced ion channel also gives rise to wiggle motion of the electrons and can lead to the realization of an X-ray laser.

1.7 Outline of the Book

We discuss these processes in subsequent chapters. In Chapter 2, we consider the properties of linear waves in a plasma. With Maxwell's equations and the equations of motion for the plasma as a starting point, we discuss the temporal and spatial dispersion and obtain expressions for the energy density and energy flow for electromagnetic and electrostatic waves in a dispersive medium. We employ Vlasov theory for electrostatic waves whereas for electromagnetic waves, a fluid description of the plasma is considered sufficient. We explain the phenomena of diffraction divergence, dispersion broadening, duct propagation, and anomalous resistivity. In Chapter 3, we study resonance absorption and Brunell absorption for electron heating. In Chapter 4, the laser coupling to surface plasmons is investigated and the phenomenon of surface enhanced Raman scattering is discussed. In Chapter 5 we study the electron response to a large amplitude electromagnetic wave and deduce an expression for the relativistic ponderomotive force for circular and linear polarizations of the laser. In Chapter 6, laser driven electron acceleration due to beat wave and wake-field mechanisms are studied. In Chapter 7, we discuss laser acceleration of quasi mono-energetic ions by radiation pressure acceleration (RPA) and target normal sheath acceleration (TNSA) mechanisms. In Chapter 8, we develop the paraxial ray theory of self-focusing of Gaussian laser beams in collisional and collisionless plasmas. For a plane uniform beam, we study the growth of the filamentation instability. Nonlinearities arise through relativistic mass variation of the electrons, the ponderomotive force, and differential Ohmic heating induced density redistribution. In Chapter 9, we study coherent radiation generation by free electron laser and ion channel X-ray lasers. Parametric instabilities in homogeneous plasma are explained in Chapter 10. We begin with the motion of a simple pendulum whose length is modulated by external means. The motion is governed by Mathieu's equation which we solve using perturbation theory. In the case of a parametric oscillator with two degrees of freedom, we solve two coupled mode equations. For plasmas, we discuss the physics of three- and four-wave parametric processes, deduce the coupled mode equations, and solve them to obtain the growth rate. Chapter 11 deals with parametric instabilities in inhomogeneous plasma. For backscattering processes, we employ the Wentzel–Kramers–Brillouin (WKB) theory that provides a convective amplification factor. For side scattering as well as for parametric instabilities near the quarter critical and critical densities, we use full wave theory to discuss convective and absolute parametric instabilities. In Chapter 12 we derive the nonlinear Schrödinger equation, and obtain steady state solitary solutions. In

https://doi.org/10.1017/9781108635844.002 Published online by Cambridge University Press

inhomogeneous plasma we study accelerating solitons, soliton excitation by lasers and the transition to chaos. In Chapter 13 we introduce particle-in-cell (PIC) and Vlasov simulations. In Chapter 14 we give an outline of high-field effects such as quantum electrodynamics (QED), and radiation reaction, and oscillating plasma mirrors.

References

1. Keldysh, L. V. 1965. "Ionization in the Field of a Strong Electromagnetic Wave." *Sov. Phys. JETP* 20 (5): 1307–1314.
2. Sharma, P., R. K. Vatsa S. K. Kulshreshtha, J. Jha, D. Mathur, and M. Krishnamurthy. 2006. "Energy Pooling in Multiple Ionization and Coulomb Explosion of Clusters by Nanosecond-Long, Megawatt Laser Pulses" *The Journal of Chemical Physics* 125 (3): 034304.
3. Rajeev, R., T. Madhu Trivikram, K. P. M. Rishad, V. Narayanan, E. Krishnakumar, and M. Krishnamurthy. 2013. "A Compact Laser-driven Plasma Accelerator for Megaelectronvolt-energy Neutral Atoms" *Nature Physics* 9 (3): 185–90.
4. C. S. Liu, M. N. Rosenbluth, and R. B. White. 1974. "Raman and Brillouin Scattering of Electromagnetic Waves in Inhomogeneous Plasmas." *The Physics of Fluids* 17 (6): 1211–19.
5. Kruer, W. L. 1988. *The Physics of Laser Plasma Interactions*. Massachusetts: Addison-Wesley.

   Jaroszynski, Dino A., R. A. Bingham, and R. A Cairns (editors). 2017. *Laser-Plasma Interactions,* 1st edition, Scottish Graduate Series. CRC Press..
6. Liu, Chuan Sheng, and V. K. Tripathi. 1986. "Parametric Instabilities in a Magnetized Plasma." *Physics Reports* 130 (3): 143–216.
7. Stix, Thomas H. 1992. *Waves in plasmas*. New York: Springer
8. Bekefi, G. 1966. *Radiation Processes in Plasmas.* New York: Wiley.
9. Ginzburg, V. L. 1970. *The Propagation of Electromagnetic Waves in Plasma.* 2nd edition. Oxford: Pergamon.
10. Nishikawa, Kyoji. 1968. "Parametric Excitation of Coupled Waves. II. Parametric Plasmon-photon Interaction." *Journal of the Physical Society of Japan* 24 (5): 1152–1158.
11. Nishikawa, Kyoji and C. S. Liu. 1976. "General Formalism of Parametric Excitation." In *Advances in Plasma Physics vol.* 6, edited by A. Simon and W. B. Thompson. p. 3; C. S. Liu and P. K. Kaw, "Parametric Instabilities in Homogeneous Unmagnetized Plasmas" *ibid.*, p. 83; C S. Liu, "Parametric Instabilities in Inomogeneous Unmagnetized Plasma" *ibid*., p. 121. New York: John Wiley.
12. Kadomtsev, Boris B., and V. I. Karpman. 1971. "Nonlinear Waves." *Soviet Physics Uspekhi* 14 (1): 40.
13. Craxton, R. S., K. S. Anderson, T. R. Boehly, V. N. Goncharov, D. R. Harding, J. P. Knauer, R. L. McCrory et al. 2015. "Direct-drive Inertial Confinement Fusion: A Review." *Physics of Plasmas* 22 (11): 110501.
14. Montgomery, David S. 2016. "Two Decades of Progress in Understanding and Control of Laser Plasma Instabilities in Indirect Drive Inertial Fusion." *Physics of Plasmas* 23 (5): 055601.

15. Lindl, John. 1995. "Development of the Indirect-drive Approach to Inertial Confinement Fusion and the Target Physics Basis for Ignition and Gain." *Physics of Plasmas* 2 (11): 3933–4024.
16. Rosenbluth, M. N., and C. S. Liu. 1972. "Excitation of Plasma Waves by Two Laser Beams." *Physical Review Letters* 29 (11): 701.
17. Tajima, Toshiki, and John M. Dawson. 1979. "Laser Electron Accelerator." *Physical Review Letters* 43 (4): 267.
18. Dahiya, Deepak, Ashok Kumar, and V. K. Tripathi. 2015. "Influence of Target Curvature on Ion Acceleration in Radiation Pressure Acceleration Regime." *Laser and Particle Beams* 33 (2): 143–149.
19. Marshall, T. C. 1985. *Free Electron Lasers.* New York: Macmillan.
20. Roberson, C. W. and P. Sprangle. 1989. "A Review of Free-Electron Lasers". *Physics of Fluids B*: *Plasma Physics* l (3): 10.1063.
21. Chen, Kuan-Ren, J. M. Dawson, A. T. Lin, and T. Katsouleas. 1991. "Unified Theory and Comparative Study of Cyclotron Masers, Ion-channel Lasers, and Free Electron Lasers." *Physics of Fluids B: Plasma Physics* 3 (5): 1270–1278.
22. Flyagin, V. A., A. V. Gaponov, I. Petelin, and V. K. Yulpatov. 1977. "The Gyrotron." *IEEE Transactions on Microwave Theory and Techniques* 25 (6): 514–521.
23. Walsh, J. E. 1980. "Cerenkov and Cerenkov–Raman Radiation Sources in Free-electron Generators of Coherent Radiation." *Phys. of Quant. Electron, vol.* 7, edited by S. F. Jacobs, H. S. Pilloff, M. Sargent III, M. O. Scully and R. Spitzer. Massachusetts: Addison-Wesley p. 255.
24. Sprangle, Phillip. 1976. "Excitation of Electromagnetic Waves from a Rotating Annular Relativistic E-beam." *Journal of Applied Physics* 47 (7): 2935–2940.